

We are IntechOpen, the world's leading publisher of Open Access books Built by scientists, for scientists

6,900

Open access books available

186,000

International authors and editors

200M

Downloads

Our authors are among the

154

Countries delivered to

TOP 1%

most cited scientists

12.2%

Contributors from top 500 universities



WEB OF SCIENCE™

Selection of our books indexed in the Book Citation Index
in Web of Science™ Core Collection (BKCI)

Interested in publishing with us?
Contact book.department@intechopen.com

Numbers displayed above are based on latest data collected.
For more information visit www.intechopen.com



Robust Control of Crane with Perturbations

Yiming Wu, He Chen and Tong Yang

Additional information is available at the end of the chapter

<http://dx.doi.org/10.5772/intechopen.71383>

Abstract

In the presence of persistent perturbations in both unactuated and actuated dynamics of crane systems, an observer-based robust control method is proposed, which achieves the objective of trolley positioning and cargo swing suppression. By dealing with the unactuated and unknown perturbation as an augmented state variable, the system dynamics are transformed into a quasi-chain-of-integrators form based on which a reduced-order augmented-state observer is established to recover the perturbations appearing in the unactuated dynamics. A novel sliding manifold is constructed to improve the robust performance of the control system, and a linear control law is presented to make the state variables stay on the manifold in the presence of perturbations in unactuated dynamics. A Lyapunov function candidate is constructed, and the entire closed-loop system is proved rigorously to be exponentially stable at the equilibrium point. The effectiveness and robustness of the proposed observer-based robust controller are verified by numerical simulation results.

Keywords: underactuated systems, overhead cranes, observer-based control, Lyapunov methods, motion control

1. Introduction

Underactuated systems [1–9] are now widely applied in modern industry. A crane system is a typical class of underactuated systems with strong state coupling. Due to inertia, when the trolley moves, the unactuated cargo swings back and forth, which affects the transporting efficiency and safety. Therefore, on the one hand, effective controllers are needed to transport the actuated trolley to desired positions. On the other hand, it is also necessary to eliminate residual vibrations of the unactuated cargo. Nevertheless, control problems of crane systems are still non-trivial and challenging since the system is underactuated without enough available control inputs.

In order to tackle control problems of crane systems, various control methods are proposed [10–38]. Specifically, Sun et al. [10, 11] present anti-swing controllers to regulate the cargo position to the desired location asymptotically in the presence of ship roll and heave movements for offshore crane systems applied in modern ocean transportation and logistics. Moreover, existing methods also include input shaping [12–15], feedback control [16–28], intelligent control [29–32], and trajectory planning method [33–36]. Specifically, several input shapers are designed to reduce payload swing of bridge crane systems [12–15]. In Ref. [16], an energy-based output feedback control scheme is proposed, which achieves both precise trolley positioning and efficient payload swing elimination under control input constraints. In Ref. [17], a payload motion-based control approach is presented in the presence of system parameter uncertainties. In [18–20], non-linear controllers are designed on the basis of partial feedback linearization. In Ref. [21], visual feedback technology is used to achieve the control objective by using two handy cameras. Additionally, sliding mode control strategies are also widely applied to tackle crane system control problems [22–25]. For example, Almutairi and Zribi [22] achieved the asymptotic stability of the closed-loop overhead crane system by proposing a sliding mode control scheme. Xi and Hesketh [23] addressed an integral sliding mode control method for discrete time crane systems with both matched and unmatched uncertainties to ensure the existence of sliding mode in the presence of uncertainties. Based on second-order sliding modes, Bartolin et al. [24] guaranteed a fast and precise payload transferring and swing suppression. Ngo and Hong [25] developed an adaptation law with a varying control gain that transits the system into the designed sliding mode. Moreover, in practical applications, cranes always suffer from unknown or uncertain system parameters (e.g., payload weight changes, varying rope lengths, etc.). Then adaptive control schemes are applied to address these problems [26–28]. Sun et al. [26] addressed the crane anti-swing and positioning problem in the presence of payload hoisting/lowering and uncertain parameters with simultaneous payload weight identification. Park et al. [27] proposed an adaptive sliding-mode anti-sway control law with system uncertainties and high-speed hoisting motion. Sun et al. [28] designed an adaptive control scheme to deal with the control problem of tower crane systems with parametric uncertainties without approximating the non-linear dynamics. There are also some intelligent control methods applied in crane systems such as fuzzy control [29, 30], genetic algorithm [31], and neural network [32]. According to the operating experience of real cranes, it is also essential to design suitable trajectories for the system states (positions, velocities, and accelerations). Then, tracking controllers can be used to track the trajectories. In addition to closed-loop control design, many studies also focus on the trajectory planning part and achieve meaningful results [33–36]. Uchiyama et al. [33] generated an S-curve trajectory numerically, which can suppress the residual vibration without measuring it. Sun et al. [34] obtained an analytical three-segment acceleration trajectory. For given transferring task, the proposed trajectory planning method provides a mechanism to determine the parameters to ensure that all the transportation indexes are met. More recently, in Ref. [35], an optimal trajectory is generated with optimal energy consumption by using the proposed optimal planner. There are also anti-swing control strategies proposed for double pendulum cranes [37, 38].

However, most of the existing methods for underactuated crane systems tackle the control problem without considering the perturbations in the unactuated dynamics. In practical applications, perturbations widely exist in both actuated and unactuated dynamics, which

may be difficult to tackle by using existing methods. Note that in Ref. [23], integral sliding mode control method is proposed by considering perturbations in unactuated dynamics, but it is only designed for discrete-time systems by estimating the present disturbance signal with its past value. Therefore, in order to derive an effective method to achieve crane control in the presence of unknown persistent (even non-vanishing) perturbations in both unactuated and actuated dynamics, this chapter proposes an observer-based robust control method.

The main contribution of this chapter is as follows:

1. According to whether the perturbation in the unactuated dynamics is vanishing or not, the control problem is stated in two cases. The observer-based robust controller designed in this chapter can achieve the control objectives for both cases.
2. By dealing with the unactuated and unknown perturbation as an augmented state variable, an augmented error system is established based on which we design a reduced-order augmented state observer for the crane system to recover the perturbations appearing in the unactuated dynamics.
3. Together with the observer, by constructing a new sliding manifold, a new observer-based sliding mode controller is developed.

The proposed controller is applicable to crane systems with unknown persistent perturbations in the unactuated dynamics and achieves robust control effectively.

The rest of this chapter is organized as follows. Section 2 describes the crane dynamics with persistent (even non-vanishing) perturbations and transforms the dynamics into a quasi-chain-of-integrators form for the convenience of controller design and stability analysis. Also, the control objective is stated in Section 2. Based on the model in Section 2, a reduced-order augmented-state observer and an observer-based control law are developed in Section 3. Then in Section 4, numerical simulation results are included to verify the effectiveness of the proposed controller. Section 5 summarizes the entire work of this chapter.

2. Problem formulation

The purpose of this chapter is to propose an effective method to achieve crane control in the presence of persistent (even non-vanishing) perturbations in both unactuated and actuated dynamics. The crane dynamics can be represented by the following equations (shown in **Figure 1**):

$$(M + m)\ddot{x} + mL\ddot{\theta} \cos\theta - mL\dot{\theta}^2 \sin\theta = u - f_r + d_x \quad (1)$$

$$mL^2\ddot{\theta} + mL \cos\theta \ddot{x} + mgL \sin\theta = d_\theta \quad (2)$$

The system parameters are defined in **Table 1**, and f_r denotes the rail friction force expressed as follows:

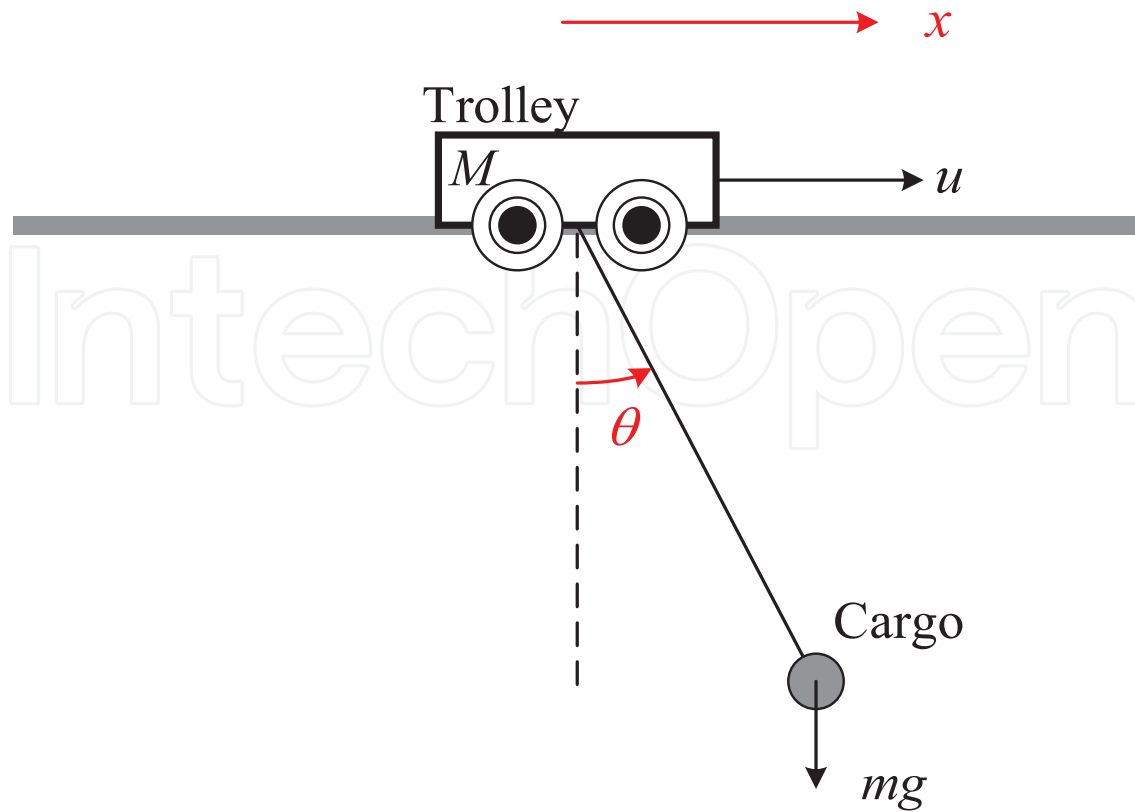


Figure 1. The schematic diagram of an overhead crane system.

$$f_r = f_{r0} \tanh(\dot{x}/\epsilon) - k_r |\dot{x}| \dot{x}, \quad (3)$$

where f_{r0} , ϵ , $k_r \in \mathbf{R}$ are friction parameters, which can be identified by offline experimental tests and data fitting. $d_x(t)$ and $d_\theta(t)$ denote the lumped term comprising external perturbations, unmodeled dynamics, the mismatch between the real girder friction and the friction compensation model shown in Eq. (3), and so forth.

System parameter	Physical significant	Unit
M	Trolley mass	kg
m	Cargo mass	kg
L	Cargo rotation radius	m
g	Gravity constant	m/s ²
x	Trolley translational displacement	m
θ	Cargo rotational angle	rad
u	Control input	N

Table 1. The system parameters of crane systems.

Considering the practical physical constraints, though the exact expressions for the lumped perturbation terms $d_x(t)$ and $d_\theta(t)$ are unknown, the following assumptions are reasonably made.

Assumption 1: The perturbation term $d_x(t)$ present in the actuated dynamics is bounded as $|d_x(t)| \leq \bar{d}_x$, where \bar{d}_x is a priori known. The unactuated perturbation term $d_\theta(t)$ is differentiable up to the n -th order; $|d_\theta| \leq \bar{d}_\theta$, $|d_\theta^{(i)}(t)| \leq \bar{d}_{\theta^{(i)}}$, $i = 1, 2, \dots, n-1$, where \bar{d}_θ and $\bar{d}_{\theta^{(i)}}$ are priori known constants. It is also assumed that $d_\theta^{(3)}(t) \approx 0$.

2.1. Crane model transformation

Before proceeding to describe the control objective, we perform several steps of transformations for the original crane dynamics shown in Eqs. (1) and (2) for the convenience of carrying out controller development and stability analysis in the subsequent section. Considering the fact of $mL > 0$, we divide both sides of Eq. (2) and make some arrangements to obtain the following equation:

$$\ddot{x} = -g \tan \theta - \frac{L\ddot{\theta}}{\cos \theta} + \frac{d_\theta}{mL \cos \theta}. \quad (4)$$

Then one can substitute Eq. (4) into Eq. (1) and make some arrangements to obtain

$$-\frac{(M+m \sin^2 \theta)L}{\cos \theta}(\ddot{\theta} - \delta_x - \delta_{\theta a}) - mL \dot{\theta}^2 \sin \theta - (M+m)g \tan \theta = u - f_r, \quad (5)$$

where $\delta_x(t)$ and $\delta_{\theta a}(t)$ are defined as follows:

$$\delta_x = -\frac{d_x \cos \theta}{(M+m \sin^2 \theta)L}, \quad \delta_{\theta a} = -\frac{d_\theta(M+m)}{(M+m \sin^2 \theta)mL^2}. \quad (6)$$

Based on *Assumption 1*, the upper bounds for $\delta_x(t)$ and $\delta_{\theta a}(t)$ are provided as:

$$|\delta_x| \leq \bar{\delta}_x = \frac{\bar{d}_x}{ML}, \quad |\delta_{\theta a}| \leq \bar{\delta}_{\theta a} = \frac{\bar{d}_\theta(M+m)}{MmL^2}. \quad (7)$$

In the view of the explicit expression of Eq. (5), a feedback linearization controller can be proposed as follows:

$$u = -\frac{(M+m \sin^2 \theta)L}{\cos \theta}v - mL \dot{\theta}^2 \sin \theta - (M+m)g \tan \theta + f_r, \quad (8)$$

in which $v(t)$ is a to-be-elaborated auxiliary control input. That is, once we derive the expression of $v(t)$, the ultimate controller $u(t)$ can be conveniently obtained according to Eq. (8). By substituting Eq. (8) into Eq. (5), together with Eq. (4), the dynamic Eqs. (1) and (2) can be re-expressed in the following fashion:

$$\begin{cases} \ddot{x} = -g \tan \theta - \frac{L\ddot{\theta}}{\cos \theta} + \frac{d_\theta}{mL \cos \theta} \\ \ddot{\theta} = v + \delta_x + \delta_{\theta a}. \end{cases} \quad (9)$$

Further, we define the following coordinate transformations:

$$\begin{aligned}\phi_1 &= x + L \ln(\sec \theta + \tan \theta) \\ \phi_2 &= x + L \dot{\theta} \sec \theta \\ \phi_3 &= -g \tan \theta \\ \phi_4 &= -g \dot{\theta} \sec^2 \theta\end{aligned}\quad (10)$$

Then, it is straightforward to obtain the following dynamic equations:

$$\begin{aligned}\dot{\phi}_1 &= \phi_{2'} \\ \dot{\phi}_2 &= \phi_3 - h(\phi_3) \phi_4^2 + \frac{d_\theta}{mL \cos \theta'} \\ \dot{\phi}_3 &= \varphi_{4'} \\ \dot{\phi}_4 &= -g(v + \delta_x + \delta_{\theta a}) \sec^2 \theta - 2g \dot{\theta}^2 \sec^2 \theta \tan \theta.\end{aligned}\quad (11)$$

In Eq. (11), the function $h(\phi_3)$ is with the definition as $h(\phi_3) = \frac{l\phi_3}{(g^2 + \phi_3^2)^{1.5}} \Rightarrow |h(\phi_3)| \leq 0.004L$, where the value of the gravity constant is taken as $g = 9.8 \text{ m/s}^2$.

For practical applications, the cargo swing is always within 10 degrees, that is, $|\theta(t)| \leq \pi/18$ rad. In this case, the approximations of $\sin \theta \approx \tan \theta \approx \theta$ and $\sec \theta = \cos^{-1} \theta \approx 1$ are valid. In this sense, $\phi_1(t)$ in Eq. (10) can be approximated as follows:

$$\phi_1(t) \approx x + L \ln(1 + \theta) \approx x + L\theta, \quad (12)$$

which is right at the horizontal position of the cargo. Also, the cargo swing angular velocity satisfies $|\dot{\theta}(t)| < 1 \text{ rad/s}$; considering that the wire length L 's order of magnitude is usually 10 m, $h(\phi_3)\phi_4^2 = 0.004Lg^2\dot{\theta}^2 \sec^4 \theta \approx 0.384L\dot{\theta}^2 \sec^4 \theta \approx 0$ holds; hence, $h(\phi_3)\phi_4^2$ is negligible and can be incorporated as part of the unactuated lumped perturbation $\delta_{\theta u}(t)$ that will be introduced later. For simplicity of denotation, we define

$$\varphi_1 = x + L\theta, \varphi_2 = \dot{\phi}_1. \quad (13)$$

Therefore, the crane dynamics can be described by

$$\begin{cases} \dot{\varphi}_1 = \varphi_{2'} \\ \dot{\varphi}_2 = \phi_3 + \delta_{\theta u'} \\ \dot{\varphi}_3 = \phi_{4'} \\ \dot{\varphi}_4 = -g(v + \delta_x + \delta_{\theta a}) \sec^2 \theta - 2g \dot{\theta}^2 \sec^2 \theta \tan \theta, \end{cases} \quad (14)$$

wherein $\delta_{\theta u}(t)$ represents the unactuated lumped perturbation term mainly consisting of $d_\theta/mL \cos \theta$.

2.2. Control objective

For crane control during the transportation process (between the hoisting and lowering stages), the kernel objective is to transfer the cargo from its initial position to the desired position (destination) and then keep it stationary right above the destination so that further actions (e.g., lowering) can be taken.

Hence, the preliminary task is to make the cargo reach the destination by appropriately controlling the trolley motion, which can be mathematically depicted as follows:

$$\varphi_1 = x + L\theta \rightarrow p_{dx}. \quad (15)$$

To make this process smooth enough, instead of set-point control (i.e., directly using p_{dx} as the reference), we want the cargo to follow a smooth time-varying trajectory $r_x(t)$, which satisfies the following conditions:

$$\lim_{t \rightarrow t_{f1}} r_x(t) = p_{dx} \mid r_x^{(i)} \mid \leq \pi, i = 1, 2, 3, 4, \quad (16)$$

where t_{f1} denotes the consumed time for $r_x(t)$ to reach p_{dx} , and $\pi_i (i = 1, 2, 3, 4)$ stands for the corresponding upper bound for the i -th order derivative for $r_x(t)$, respectively.

When there are no external perturbations appearing in the unactuated dynamics (that is, $\delta_{\theta u} \equiv 0$ in Eq. (14)), we need also to damp out the cargo swing $\theta(t)$ at the same time, namely,

$$\theta \rightarrow 0 \Rightarrow x \rightarrow p_{dx}. \quad (17)$$

However, in the case of persistent, non-vanishing perturbations in the unactuated component (i.e., $\delta_{\theta u}(t) \neq 0$), there *does not exist any control action* that can completely damp out $\theta(t)$ while keeping the cargo stationary right above the destination. Suppose that there exists such a controller $u'(t)$ that could eliminate the cargo swing, namely,

$$\theta(t) = 0, \dot{\theta}(t) = 0 \Rightarrow \phi_3(t) = -g \tan \theta(t) = 0, \quad (18)$$

and make the cargo stay stationary at the destination in the sense that

$$\varphi_1(t) = p_{dx}, \dot{\varphi}_1(t) = 0, \varphi_2(t) = 0, \dot{\varphi}_2(t) = 0, \forall t \geq t_{f2}, \quad (19)$$

with t_{f2} being the settling time, then it would follow, by inserting Eq. (18) and Eq. (19) into the second equation of Eq. (14), that

$$\delta_{\theta u} = \dot{\varphi}_2 - \dot{\phi}_3 = 0, \quad (20)$$

which obviously contradicts with the fact that $\delta_{\theta u} \neq 0$; thus the existence of such a controller $u'(t)$ is impossible. This fact illustrates the great challenge that will be faced with when

controlling the crane system in the presence of persistent perturbations in the unactuated dynamics. On the other hand, since $\delta_{\theta u}(t)$ is usually unknown, the control problem becomes even more challenging.

Based on the analysis claimed above, in accordance with the fact whether $\delta_{\theta u}$ in the unactuated dynamics is vanishing or not, the control objective of this chapter is stated as follows:

- **Case 1.** *Non-vanishing perturbations in the unactuated dynamics.* Drive the unactuated cargo to the desired destination and keep it stationary over the destination thereafter, that is,

$$\lim_{t \rightarrow \infty} \varphi_1(t) = p_{dx'} \lim_{t \rightarrow \infty} \dot{\varphi}_1(t) = 0. \quad (21)$$

- **Case 2.** *Vanishing or no/negligible perturbations in the unactuated dynamics.* Drive both the trolley and the unactuated cargo to the desired destination, in the sense that

$$\lim_{t \rightarrow \infty} \varphi_1(t) = p_{dx'} \lim_{t \rightarrow \infty} x(t) = p_{dx'} \lim_{t \rightarrow \infty} \dot{\varphi}_1(t) = 0, \lim_{t \rightarrow \infty} \dot{x} = 0 \Rightarrow \lim_{t \rightarrow \infty} \theta(t) = 0, \lim_{t \rightarrow \infty} \dot{\theta}(t) = 0. \quad (22)$$

To achieve the control objective, together with Eq. (16), let the following error signals be defined:

$$e_1 = \varphi_1 - r_{x'}, e_2 = \varphi_2 - r_{x'}, e_3 = \phi_{3'} e_4 = \phi_4. \quad (23)$$

Thus, we are led to the following open-loop error system:

$$\begin{cases} \dot{e}_1 = e_{2'} \\ \dot{e}_2 = e_3 + \delta_{\theta u} - \dot{r}_{x'} \\ \dot{e}_3 = e_{4'} \\ \dot{e}_4 = -g(v + \delta_x + \delta_{\theta u}) \sec^2 \theta - 2g \dot{\theta}^2 \sec^2 \theta \tan \theta, \end{cases} \quad (24)$$

which is the basis for the observer-controller design and analysis in the section that follows.

3. Main results

In order to achieve the control objective claimed in the previous section, we will propose a perturbation observer-based robust control scheme. More precisely, to deal with the unactuated unknown persistent perturbations, an augmented-state observer will be constructed. Then, we will present a novel robust control law, which can achieve superior control performance and provide the corresponding theoretical stability analysis.

3.1. Observer design

The fact that the perturbation term $\delta_{\theta u}(t)$ is *unactuated and unknown* brings much difficulty for the controller design and analysis and it makes traditional robust control methods not

applicable. As a means to achieve the aforementioned control objective, it is required to figure out a suitable strategy that can deal with $\delta_{\theta u}(t)$. Toward this end, before controller development, we will first construct an augmented observer which can recover the lumped perturbation term $\delta_{\theta u}(t)$ appearing in the unactuated dynamics. Then, we treat $\delta_{\theta u}(t)$ as an augmented state variable. The benefit of doing so is that the perturbation observer design procedure would become more concise and clear. By following this line, the augmented error system for Eq. (24) is established as follows:

$$\begin{cases} \dot{e}_1 = e_2, \\ \dot{e}_2 = e_3 + e_5 - \ddot{r}_x, \\ \dot{e}_3 = e_4, \\ \dot{e}_4 = -g(v + \delta_x + \delta_{\theta a}) \sec^2 \theta - 2g \theta^2 \sec^2 \theta \tan \theta, \\ \dot{e}_5 = e_6, \\ \dot{e}_6 = e_7, \\ \vdots \\ \dot{e}_{n+1} = 0, \\ y = e_1 \end{cases} \quad (25)$$

where we have considered $\delta_{\theta u}(t)$ as an augmented state variable $e_5(t)$ and its derivatives as $e_6(t), e_7(t), \dots, e_{n+1}(t)$, and $y(t)$ is the corresponding system output signal. In this chapter, the signals $e_1(t), e_3(t)$ and $e_4(t)$ are measurable, and we merely need to fabricate an observer with the aim of recovering the lumped perturbation $e_5(t)$. In order to reduce the computational complexity, noting also that $\theta_x(t)$ and $\theta_{\theta a}(t)$ are unavailable for feedback, we intend to construct a reduced-order perturbation observer. For this purpose, consider the following subsystem:

$$\begin{cases} \dot{e}_2 = e_3 + e_5 - \ddot{r}_x, \\ \dot{e}_5 = e_6, \\ \dot{e}_6 = e_7, \\ \vdots \\ \dot{e}_{n+1} = 0, \\ y' = e_2 \end{cases} \quad (26)$$

which is part of the augmented error system shown in Eq. (25), where $y'(t)$ is regarded as the new output. It is not difficult to check that the reduced-order augmented-state system shown in Eq. (26) is observable, and the detailed analysis can be found in Appendix A. Based on the structure of Eq. (26), we design the following reduced-order augmented-state observer:

$$\begin{cases} \dot{\hat{e}}_2 = e_3 + \hat{e}_5 - \ddot{r}_x - \lambda_2(\hat{e}_2 - y'), \\ \dot{\hat{e}}_5 = \hat{e}_6 - \lambda_5(\hat{e}_2 - y'), \\ \dot{\hat{e}}_6 = \hat{e}_7 - \lambda_6(\hat{e}_2 - y'), \\ \vdots \\ \dot{\hat{e}}_{n+1} = -\lambda_{n+1}(\hat{e}_2 - y'), \end{cases} \quad (27)$$

where $\lambda_{2'}, \lambda_{5'}, \lambda_{6'}, \dots, \lambda_{n+1}$ denote the observer gains. Define the following error signals:

$$\xi_i = \hat{e}_i - e_i, i = 2, 5, 6, \dots, n+1, \quad (28)$$

and denote the corresponding error vector by

$$\xi(t) = [\xi_2(t) \ \xi_5(t) \ \xi_6(t) \ \dots \ \xi_{n+1}(t)]^\top. \quad (29)$$

Then, one can subtract Eq. (26) from Eq. (27) to derive the following observer error system:

$$\dot{\xi} = \Omega \xi, \quad (30)$$

where $\Omega \in \mathbf{R}^{(n-2) \times (n-2)}$ is defined as:

$$\Omega = \begin{pmatrix} -\lambda_2 & 1 & 0 & \dots & 0 & 0 \\ -\lambda_5 & 0 & 1 & \dots & 0 & 0 \\ -\lambda_6 & 0 & 0 & \ddots & 0 & 0 \\ \vdots & \vdots & \vdots & \vdots & \ddots & \vdots \\ -\lambda_n & 0 & 0 & \dots & 0 & 1 \\ -\lambda_{n+1} & 0 & 0 & \dots & 0 & 0 \end{pmatrix}. \quad (31)$$

As stated previously, the system shown in Eq. (26) is observable. Hence, without difficulty, we are admitted to choose a proper set of $\lambda_{2'}, \lambda_{5'}, \lambda_{6'}, \dots, \lambda_{n+1}$ conveniently via pole placement, such that Ω is a Hurwitz matrix with *the eigenvalues' real parts being different from each other*. In this sense,

$$\xi_i = \hat{e}_i - e_i \rightarrow 0, i = 2, 5, 6, \dots, n+1, \quad (32)$$

exponentially fast, which indicates that the designed perturbation observer shown in Eq. (27) can online recover the perturbations.

In addition, it can be obtained from Eq. (30) that the trajectories of the observer error signals are represented by

$$\xi = \exp(\Omega t) \xi(0). \quad (33)$$

Since we have rendered, by proper pole placement, that the poles (i.e., the eigenvalues of Ω) of the closed-loop system shown in Eq. (30) have different negative real parts, there exists an invertible matrix $\Gamma \in \mathbf{R}^{(n-2) \times (n-2)}$ that can transform Ω into a diagonal matrix, that is,

$$\Gamma^{-1} \Omega \Gamma = \Lambda, \quad (34)$$

where $\Lambda = \text{diag} \{\lambda_{1'}, \lambda_{2'}, \dots, \lambda_{n-2}\}$ with $\lambda_{i'}, i = 1, 2, \dots, n-2$ being the $(n-2)$ eigenvalues of Γ . Therefore, we can rewrite the exponential matrix $\exp(\Omega t)$ and $\xi(t)$ as [39]

$$\exp(\Omega t) = \Gamma \exp(\Lambda t) \Gamma^{-1} \Rightarrow \xi = \Gamma \exp(\Lambda t) \Gamma^{-1} \xi(0). \quad (35)$$

Taking the Euclidean norm for both sides of Eq. (35), we are led to the following results:

$$\begin{aligned} \|\xi\|_2 &= \|\Gamma \exp(\Lambda t) \Gamma^{-1} \xi(0)\|_2 \leq \|\Gamma \exp(\Lambda t) \Gamma^{-1}\|_{m_\infty} \cdot \|\xi(0)\|_2 \\ &\leq \|\Gamma\|_{m_\infty} \cdot \|\Gamma^{-1}\|_{m_\infty} \cdot \|\exp(\Lambda t)\|_{m_\infty} \|\xi(0)\|_2 \leq (n-2) \exp(\lambda_{\max} t) \cdot \|\Gamma\|_{m_\infty} \cdot \|\Gamma^{-1}\|_{m_\infty} \cdot \|\xi(0)\|_2 \end{aligned} \quad (36)$$

where $\lambda_{\max} = \max_{i=1,2,\dots,n-2} \{\lambda_i\}$, $\|\cdot\|_2$ denotes the Euclidean norm, $\|\cdot\|_{m_\infty}$ represents the m_∞ -norm for matrices¹, which are compatible norms². It is further implied from Eq. (36) that

$$|\xi_i(t)| \leq \|\xi\|_2 \leq \bar{\xi} \triangleq (n-2) \exp(\lambda_{\max} t) \cdot \|\Gamma\|_{m_\infty} \cdot \|\Gamma^{-1}\|_{m_\infty} \cdot \|\xi(0)\|_2. \quad (37)$$

Using the pole assignment technique, one can derive the values for $\lambda_{2'}, \lambda_{3'}, \lambda_{4'}, \dots, \lambda_{n+1}$ and the expression for Ω . Further, with the aid of such software as MATLAB, it is easy to calculate $\|\Gamma\|_{m_\infty} \cdot \|\Gamma^{-1}\|_{m_\infty}$; hence, the bound for $|\xi_i(t)|$, as shown in Eq. (37), can be computed without difficulty.

3.2. Controller development and stability analysis

To achieve robust control in the presence of uncertainties or external perturbations, we will develop a new observer-based sliding mode controller. The fundamental idea of the sliding mode control method is to construct a sliding manifold (surface) on which the system state is convergent and then develop a suitable control law that renders the state reaches the manifold within finite time. Traditionally, the key step is constructing an appropriate sliding surface, and the corresponding controller can usually be obtained straightforwardly.

However, the major drawback of most currently available sliding mode control methods is that they are merely capable of tackling uncertainties or perturbations in the actuated part, and when uncertainties or perturbations are present in the unactuated component, their performance will degrade significantly and even become unstable. To illustrate this point, we will show some brief analysis for the conventional sliding mode control approach. More precisely, for the open-loop error system shown in Eq. (24), one will design the conventional sliding manifold, denoted by $\zeta(t)$ in the following fashion:

$$\zeta = e_1 + \alpha e_2 + \beta e_3 + \gamma e_4 \quad (38)$$

where α, β , and γ are sliding slopes chosen such that the polynomial $1 + \alpha s + \beta s^2 + \gamma s^3 = 0$ is Hurwitz, with s being the complex variable. It is not difficult to design a control law that drives the system state variables to $\zeta(t)$ such that $\zeta(t) = 0$ after certain finite time t_s , i.e., $\zeta(t) = 0, \forall t \geq t_s$. By recursively using the first three equations in Eq. (24) and regrouping the

¹For a square matrix $A = (a_{ij})_{n \times n} \in \mathbf{R}^{n \times n}$, $\|A\|_{m_\infty} = n \max_{i,j} |a_{ij}|$ is defined as the m_∞ -norm for A .

²A matrix norm $\|\cdot\|_m \in \mathbf{R}^{n \times n}$ is said to be compatible with a vector norm $\|\cdot\|_v \in \mathbf{R}^n$ if $\|Ax\|_v \leq \|A\|_m \cdot \|x\|_v$, where $A \in \mathbf{R}^{n \times n}$ and $x \in \mathbf{R}^n$. It is not difficult to verify that the m_∞ -norm for matrices is compatible with the Euclidean norm for vectors.

resulting terms, one can derive from $\zeta(t)=0$ and Eq. (38) that the state variable $e_1(t)$ is dominated by the following dynamics on the sliding manifold:

$$e_1 + \alpha \dot{e}_1 + \beta \ddot{e}_1 + \gamma e_1^{(3)} = -\beta(\ddot{r}_x - \delta_{\theta u}) - \gamma(r_x^{(3)} - \delta_{\theta u}). \quad (39)$$

Clearly, if the perturbation terms $\delta_{\theta u}(t), \delta_{\theta u}(t)$ appearing in the unactuated dynamics are non-vanishing, $e_1(t)$ will never tend to zero.

As indicated from the above-mentioned analysis, to make sliding mode control applicable to crane systems with *unknown persistent perturbations* in the unactuated component, it is needed to construct a new sliding manifold to improve the robust performance of the control system. To do so, on the basis of the designed perturbation observer in the previous subsection, we design the following sliding manifold that will be used in the subsequent controller development:

$$\varepsilon = e_1 + \alpha e_2 + \beta(e_3 + \hat{e}_5 - \ddot{r}_x) + \gamma(e_4 + \hat{e}_6 - r_x^{(3)}). \quad (40)$$

where α, β, γ are defined in Eq. (38) and $\hat{e}_5(t), \hat{e}_6(t)$ are the observer-recovered signals for the lumped perturbation term [see Eq. (27)]. Before giving the expression for the auxiliary “control input” $v(t)$, we first construct the following non-negative scalar function $V(t)$:

$$V = \frac{1}{2} \varepsilon^2 = \frac{1}{2} [e_1 + \alpha e_2 + \beta(e_3 + \hat{e}_5 - \ddot{r}_x) + \gamma e_4(e_4 + \hat{e}_6 - r_x^{(3)})]^2. \quad (41)$$

The derivative of $\varepsilon(t)$ with regard to time can be obtained as follows:

$$\begin{aligned} \dot{\varepsilon} = & e_2 + \alpha(e_3 + \dot{e}_5 - \ddot{r}_x) + \beta[e_4 + \dot{\hat{e}}_6 - \lambda_5(\hat{e}_2 - e_2) - r_x^{(3)}] - \gamma g(v + \delta_x + \delta_{\theta u}) \sec^2 \theta \\ & - \gamma [2g \theta^2 \sec^2 \theta \tan \theta - \dot{\hat{e}}_7 + \lambda_6(\hat{e}_2 - e_2) + r_x^{(4)}], \end{aligned} \quad (42)$$

where Eq. (25) and Eq. (27) have been employed for implications. Then, in view of the structure of Eq. (42), $v(t)$ is developed in the following fashion:

$$\begin{aligned} v = & \frac{1}{g \gamma \sec^2 \theta} \cdot \{e_2 + \alpha(e_3 + \dot{\hat{e}}_5 - \ddot{r}_x) - \gamma[r_x^{(4)} - \dot{\hat{e}}_7 + \lambda_6(\hat{e}_2 - e_2)] \\ & + \beta[e_4 + \dot{\hat{e}}_6 - \lambda_5(\hat{e}_2 - e_2) - r_x^{(3)} + k_u \text{sign}(\varepsilon)]\} - 2 \dot{\theta}^2 \tan \theta + k_a \text{sign}(\varepsilon) \end{aligned} \quad (43)$$

where

$$k_a \geq \bar{\delta}_x + \bar{\delta}_{\theta'}, k_u > \frac{\alpha \bar{\xi}}{\beta}. \quad (44)$$

are positive control gains [see Eqs. (7) and (37) for the definitions of $\bar{\delta}_x, \bar{\delta}_{\theta'}$, and $\bar{\xi}$], and

$$\text{sign}(\star) = \begin{cases} \star / |\star|, & \star \neq 0, \\ 0, & \star = 0, \end{cases} \quad (45)$$

denote the standard sign function. We can further substitute Eq. (43) into Eq. (8) to obtain the ultimate control law as follows:

$$\begin{aligned}
 u = & -\frac{(M+m \sin^2 \theta)L}{g \gamma \sec \theta} \cdot \left\{ e_2 + \alpha(e_3 + \hat{e}_5 - \ddot{r}_x) - \gamma[r_x^{(4)} - \hat{e}_7 + \lambda_6(\hat{e}_2 - e_2)] \right. \\
 & + \beta[e_4 + \hat{e}_6 - \lambda_5(\hat{e}_2 - e_2) - r_x^{(3)} + k_u \text{sign}(\epsilon)] + g \gamma \sec^2 \theta [2 \theta^2 \tan \theta - k_a \text{sign}(\epsilon)] \left. \right\} \\
 & - mL \dot{\theta}^2 \sin \theta - (M+m)g \tan \theta + f_r.
 \end{aligned} \tag{46}$$

The main results for the proposed control scheme are summarized by the theorem that follows.

Theorem 1. The designed control law shown in Eq. (46), together with the reduced-order augmented-state observer shown in Eq. (27), can achieve the control objective claimed by **Case 1** in the case of unactuated persistent non-vanishing disturbances or **Case 2** if the unactuated disturbances are vanishing/negligible.

Proof: Consider $V(t)$ defined in Eq. (41) as a Lyapunov function candidate, and its time derivative is given by

$$\dot{V} = \epsilon \dot{\epsilon}. \tag{47}$$

By inserting Eq. (43) into the expression of $\dot{\epsilon}(t)$ in Eq. (42) and regrouping the common terms, one can obtain the following equation:

$$\begin{aligned}
 \dot{\epsilon} = & \alpha(e_5 - \hat{e}_5) - \beta k_u \text{sign}(\epsilon) - g \gamma \sec^2 \theta [k_u \text{sign}(\epsilon) + \delta_x + \delta_{\theta a}] \\
 = & -\alpha \xi_5 - \beta k_u \text{sign}(\epsilon) - g \gamma \sec^2 \theta [k_u \text{sign}(\epsilon) + \delta_x + \delta_{\theta a}],
 \end{aligned} \tag{48}$$

upon the use of the relationship in Eq. (28). Then, the following results are straightforward after the substitution of Eq. (48) into Eq. (47):

$$\begin{aligned}
 \dot{V} = & -\beta k_u |\epsilon| - \alpha \xi_5 \epsilon + g \gamma \sec^2 \theta [k_u |\epsilon| + (\delta_x + \delta_{\theta a}) \epsilon] \\
 \leq & -(\beta k_u - \alpha |\xi_5|) |\epsilon| - g \gamma \sec^2 \theta (k_u - (|\delta_x| + |\delta_{\theta a}|)) |\epsilon| \\
 \leq & -(\beta k_u - \alpha |\xi_5|) \sqrt{2V},
 \end{aligned} \tag{49}$$

where the gain conditions shown in Eq. (44) have been utilized. The conclusion of Eq. (49) indicates that $V(t)$, and hence $\epsilon(t)$, converges to zero in finite time. Further, on the sliding manifold where $\epsilon(t) = 0$, the system state variables satisfy the following dynamic equation array:

$$\begin{cases} e_1 + \alpha \dot{e}_1 + \beta \ddot{e}_1 + \gamma e_1^{(3)} = -\beta \xi_5 - \gamma \xi_6 \\ \dot{\xi} = \Omega \xi. \end{cases} \tag{50}$$

As by pole assignment, the matrix $\Omega \in \mathbb{R}^{(n-2) \times (n-2)}$ is Hurwitz, and α, β and γ also render $1 + \alpha s + \beta s^2 + \gamma s^3 = 0$ Hurwitz; it is clearly seen that the entire closed system Eq. (50) is exponentially stable at the equilibrium point, and hence

$$\begin{aligned} e_1(t) &= \varphi_1(t) - r_x \rightarrow 0, e_2(t) = \dot{e}_1(t) = \dot{\varphi}_1(t) - \dot{r}_x \rightarrow 0 \\ \Rightarrow \ddot{e}_2(t) &= \ddot{e}_1(t) \rightarrow 0, \ddot{e}_2(t) = e_1^{(3)}(t) \rightarrow 0, \end{aligned} \quad (51)$$

exponentially fast, which indicates the cargo motion tracks the planned trajectory $r_x(t)$ in an exponential fashion. Since $r_x(t)$ tends to p_{dx} within t_{fl} [see Eq. (16)], it is easily shown that

$$\lim_{t \rightarrow \infty} \varphi_1(t) = p_{dx} \lim_{t \rightarrow \infty} \dot{\varphi}_1(t) = 0, \quad (52)$$

which is just the result of Eq. (21). In addition, as $\dot{r}_x(t), r_x^{(3)}(t) \rightarrow 0$ as $t \rightarrow 0$ by definition [see Eq. (16)], it is implied by substituting the result of $\ddot{e}_2(t) \rightarrow 0$ into the second and third equations of Eq. (24) that

$$e_3 \rightarrow \dot{e}_2 - \delta_{\theta u} \rightarrow -\delta_{\theta u'} \dot{e}_3 \rightarrow \ddot{e}_2 - \dot{\delta}_{\theta u} \rightarrow -\dot{\delta}_{\theta u'} e_4 \rightarrow \dot{e}_3 \rightarrow -\dot{\delta}_{\theta u'} \quad (53)$$

wherein the conclusions in Eq. (52) have been employed. The results in Eq. (53) indicate that $e_3(t), \dot{e}_3(t)$ are convergent to their respective equilibriums drifted by the unactuated perturbations. Thus, the result of **Case 1** stated in the control objective is proven.

Subsequently, we proceed to prove the result of **Case 2** where the perturbation term $\delta_{\theta u}(t)$ in the unactuated dynamics is vanishing [i.e., $\delta_{\theta u} \rightarrow 0, \dot{\delta}_{\theta u} \rightarrow 0$] or negligible [i.e., $\delta_{\theta u}(t) = 0, \dot{\delta}_{\theta u}(t) = 0$]. Therefore, in such cases, it is straightforward to indicate from Eq. (53) that

$$e_3 = -g \tan \theta \rightarrow 0, e_4 = -g \theta \sec^2 \theta \rightarrow 0 \Rightarrow \theta = 0, \dot{\theta} = 0, \quad (54)$$

where the definitions in Eq. (10) and Eq. (23) have been used. According to the definition of $\varphi_1(t) = x(t) + L\theta(t)$ given in Eq. (13), the results in Eq. (52) and Eq. (54) directly yield the following conclusions:

$$\lim_{t \rightarrow \infty} x(t) = p_{dx} \lim_{t \rightarrow \infty} \dot{x}(t) = 0. \quad (55)$$

Collecting up Eqs. (52, 54, 55), the results claimed in Eq. (22) of **Case 2** are hence proven. The entire theoretical proof for the theorem is completed.

4. Simulation verification

In this section, by using the MATLAB/Simulink software, some simulation results are included to verify the effectiveness of the proposed observer-based robust control method.

For the control objectives of the two cases stated in Eq. (21) and Eq. (22), the simulation is implemented through two groups as follows:

- **Group 1.** The perturbations in the unactuated dynamics are non-vanishing. The perturbation $d_\theta(t)$ is set as a constant value $d_\theta(t) = 1$ and a time-varying function $d_\theta(t) = 0.5 \cos(0.1t)$, respectively.

- **Group 2.** The perturbations in the unactuated dynamics are vanishing or negligible. The perturbation $d_\theta(t)$ is set as a time-varying function $d_\theta(t) = 1.5e^{-t}$.

For all the cases, by setting the system parameters as $M = 6 \text{ kg}$, $m = 2.5 \text{ kg}$, $L = 1.2 \text{ m}$, $g = 9.8 \text{ m/s}^2$, the controller parameters as $\lambda_2 = 10$, $\lambda_5 = 30$, $\lambda_6 = 55$, $\lambda_7 = 25$, $\alpha = 2$, $\beta = 1$, $\gamma = 0.2$, $\varepsilon = 0.01$, $k_u = 60$, $k_a = 0.1$, and the to-be-tracked trajectory in Eq. (16) as $r_x(t) = 3.5$, the simulation results are obtained and are shown in **Figures 2–4**.

Figures 2 and **3** show the simulation results of **Group 1** where the solid lines denote the simulation results and the dash lines denote the desired trajectories. In **Figure 2**, the perturbation $d_\theta(t)$ is set as a constant value $d_\theta(t) = 1$, and in **Figure 3**, the perturbation is set as a time-varying function $d_\theta(t) = 0.5 \cos(0.1t)$. It can be seen from **Figures 2** and **3** that when there exist persistent (non-vanishing) perturbations in the unactuated dynamics, by applying the proposed controller, the unactuated cargo is driven to the desired destination and is kept stationary. Therefore, the objectives stated in **Case 1** [see Eq. (21)] are achieved effectively. By dealing with the robust control for crane systems when the perturbations are non-vanishing, the results of **Group 1** validate the robustness of the presented controller.

Figure 4 shows the results of **Group 2**. It is clear that the proposed observer-based robust control method can achieve the objectives stated in **Case 2** [see Eq. (22)] that both the trolley

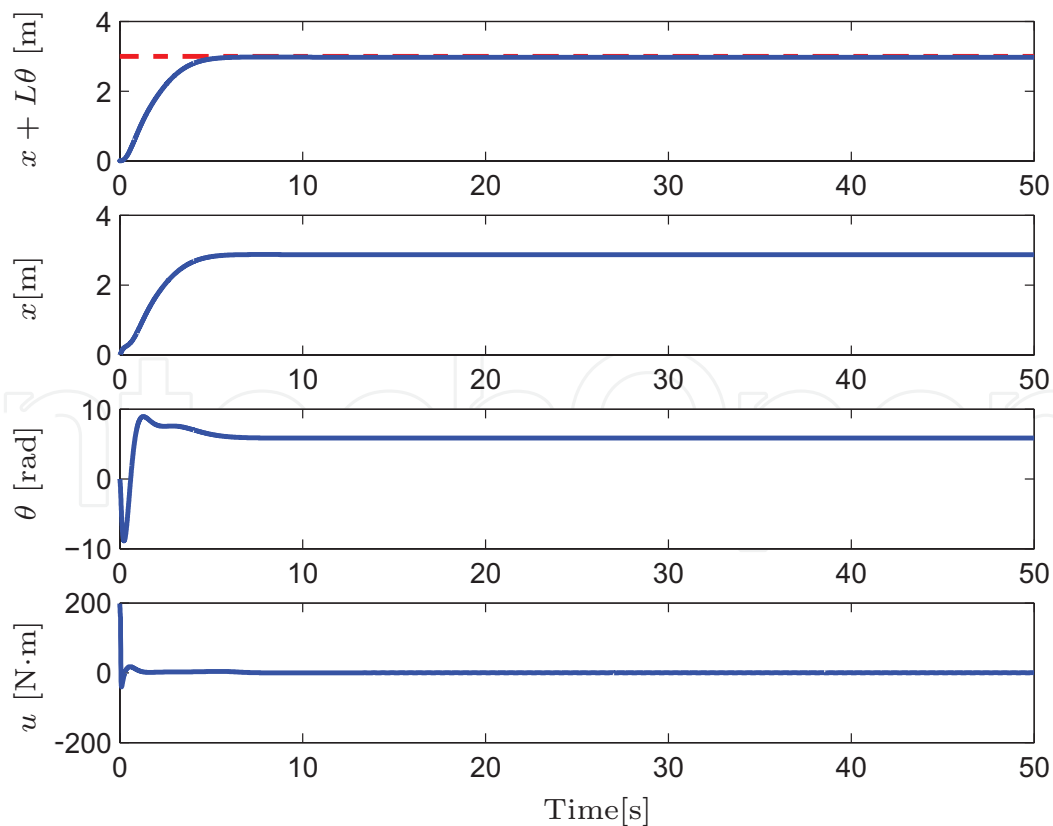


Figure 2. The simulation results of the proposed controller when $d_\theta(t) = 1$ (solid line – simulation results, dash line – desired trajectory).

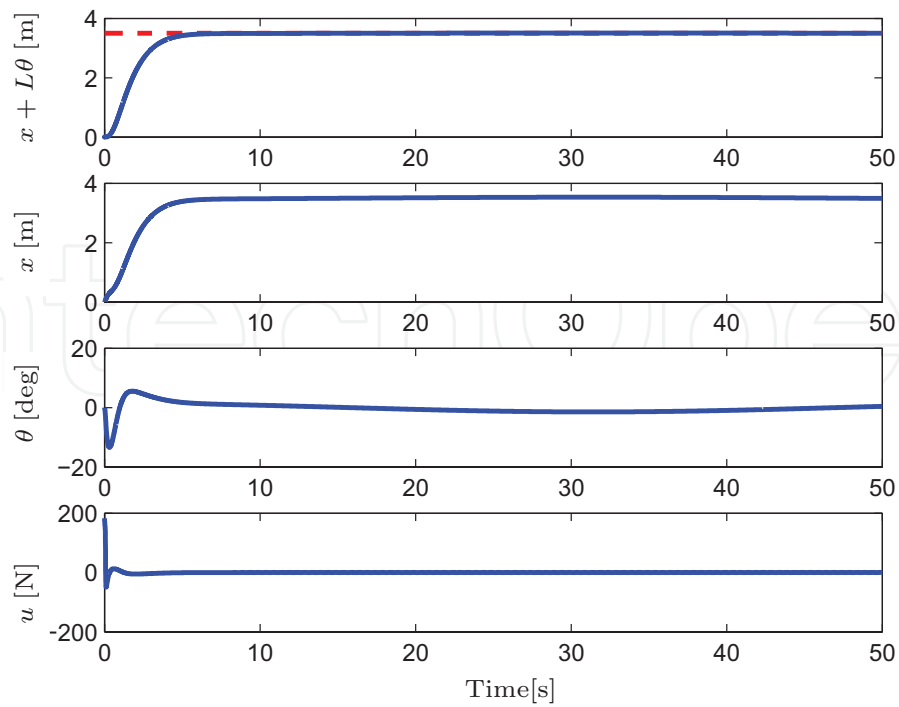


Figure 3. The simulation results of the proposed controller when $d_\theta(t) = 0.5 \cos(0.1t)$ (solid line – simulation results, dash line – desired trajectory).

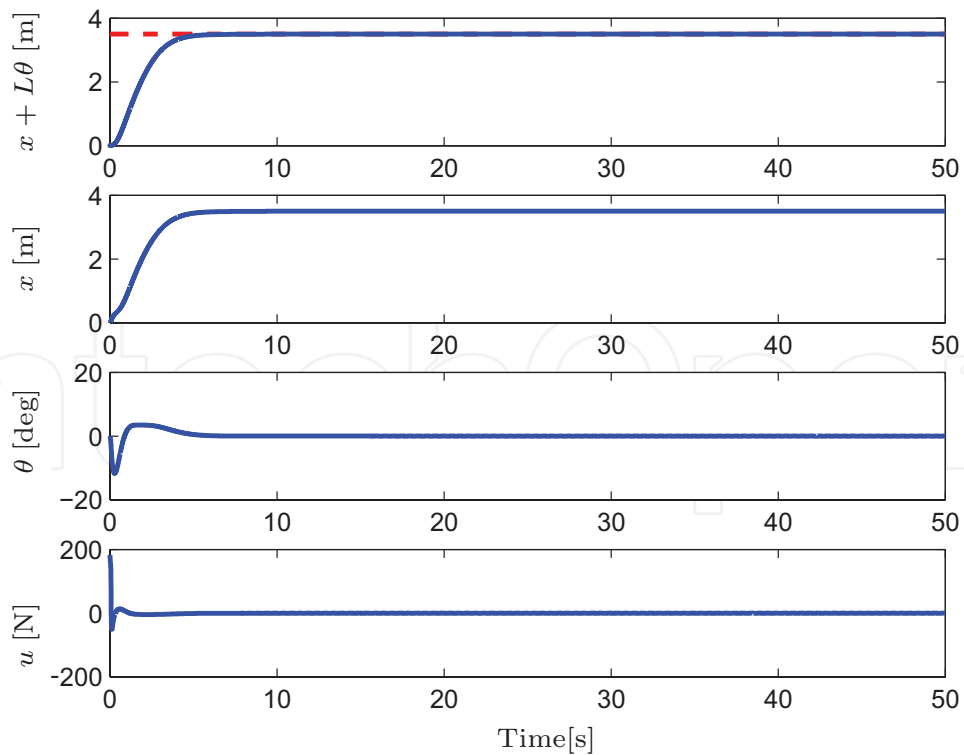


Figure 4. The simulation results of the proposed controller when $d_\theta(t) = 1.5e^{-t}$ (solid line – simulation results, dash line – desired trajectory).

and the unactuated cargo are driven to the desired destination, when there are no/negligible or vanishing perturbations $d_\theta(t) = 1.5e^{-t}$ in the unactuated dynamics.

To sum-up, the simulation results indicate that the proposed observer-based robust controller can achieve robust control in the presence of uncertainties or external perturbations, which is consistent with the theoretical analysis.

5. Concluding remarks

Considering unknown persistent perturbations in unactuated dynamics, this chapter designs an observer-based robust control method for underactuated crane systems. Specifically, a reduced-order augmented-state observer is designed to recover the lumped perturbation terms in unactuated dynamics. Further, based on the observer, a new sliding manifold is constructed to improve the robust performance of the control system. Then, the state variables are made to stay on the manifold by applying a designed robust control law in the presence of non-vanishing perturbations in unactuated dynamics. Finally, the convergence is proved in this chapter theoretically by using Lyapunov control theories. Moreover, the proposed observer-based robust controller is verified to be effective and robust by numerical simulation results.

Appendix

The system shown in Eq. (26) can be rewritten as follows:

$$\begin{aligned} \dot{\chi} &= A\chi + (e_3 - \ddot{r}_x \ 0 \ 0 \ \dots \ 0 \ 0)^T, \\ y' &= C\chi \end{aligned} \tag{56}$$

where the system variable vector $\chi(t)$ is defined as $\chi = (e_2, e_5, e_6, \dots, e_{n+1})^T$. The system parameter matrix $A \in \mathbf{R}^{(n-2) \times (n-2)}$ and $C \in \mathbf{R}^{(n-2)}$ are

$$\begin{aligned} A &= \begin{pmatrix} 0 & 1 & 0 & \dots & 0 & 0 \\ 0 & 0 & 1 & \dots & 0 & 0 \\ 0 & 0 & 0 & \dots & 0 & 0 \\ \vdots & \vdots & \vdots & & \vdots & \vdots \\ 0 & 0 & 0 & \dots & 1 & 0 \\ 0 & 0 & 0 & \dots & 0 & 1 \\ 0 & 0 & 0 & \dots & 0 & 0 \end{pmatrix}, \\ C &= (1 \ 0 \ 0 \ \dots \ 0 \ 0). \end{aligned} \tag{57}$$

Then, considering the observability criteria, we can first derive the observable matrix Ψ as follows:

$$\Psi = \begin{pmatrix} C \\ CA \\ CA^2 \\ \vdots \\ CA^{(n-3)} \end{pmatrix} = \begin{pmatrix} 1 & 0 & 0 & \cdots & 0 & 0 \\ 0 & 1 & 0 & \cdots & 0 & 0 \\ 0 & 0 & 0 & \cdots & 0 & 0 \\ \vdots & \vdots & \vdots & & \vdots & \vdots \\ 0 & 0 & 0 & \cdots & 1 & 0 \\ 0 & 0 & 0 & \cdots & 0 & 1 \\ 0 & 0 & 0 & \cdots & 0 & 0 \end{pmatrix}. \quad (58)$$

It is clear that $\Psi \in \mathbf{R}^{(n-2) \times (n-2)}$, whose rank is $\text{rank}(\Psi) = A = n - 2$. Thus, the system shown in Eq. (26) is observable.

Author details

Yiming Wu^{1,2*}, He Chen^{1,2} and Tong Yang^{1,2}

*Address all correspondence to: wuyiming_1@126.com

1 Institute of Robotics and Automatic Information Systems, College of Computer and Control Engineering, Nankai University, Tianjin, China

2 Tianjin Key Laboratory of Intelligent Robotics, Nankai University, Tianjin, China

References

- [1] Sun N, Wu Y, Fang Y, Chen H. Nonlinear stabilization control of multiple-RTAC systems subject to amplitude-restricted actuating torques using only angular position feedback. *IEEE Transactions on Industrial Electronics*. 2017;**64**(7):3084-3094
- [2] Sun N, Wu Y, Fang Y, Chen H, Lu B. Nonlinear continuous global stabilization control for underactuated RTAC systems: Design, analysis, and experimentation. *IEEE/ASME Transactions on Mechatronics*. 2017;**22**(2):1104-1115
- [3] Xin X, Liu Y. Reduced-order stable controllers for two-link underactuated planar robots. *Automatica*. 2013;**49**(7):2176-2183
- [4] Xia D, Wang L, Chai T. Neural-network friction compensation based energy swing-up control of Pendubot. *IEEE Transactions on Industrial Electron*. 2014;**61**(3):1411-1423
- [5] Cui R, Guo J, Mao Z. Adaptive backstepping control of wheeled inverted pendulums models. *Nonlinear Dynamics*. 2015;**79**(1):501-511
- [6] Yang C, Li Z, Li J. Trajectory planning and optimized adaptive control for a class of wheeled inverted pendulum vehicle models. *IEEE Transactions on Cybernetics*. 2013;**43**(1):24-36

- [7] Kato K, Wada M. Kinematic analysis and simulation of active-caster robotic drive with ball transmission (ACROBAT-S). *Advanced Robotics*. 2017;**31**(7):355-367
- [8] Oka H, Maruki Y, Suemitsu H, Matsuo T. Nonlinear control for rotational movement of cart-pendulum system using homoclinic orbit. *International Journal of Control, Automation and Systems*. 2016;**14**(5):1270-1279
- [9] Inoue Y, Hirama T, Wada M. Design of omnidirectional mobile robots with ACROBAT wheeled mechanisms. In: *IEEE/RSJ International Conference on Intelligent Robots and Systems (IROS)*, 3-7 Nov, Tokyo, Japan. 2013. p. 4852-4859
- [10] Sun N, Fang Y, Chen H, Fu Y, Lu B. Nonlinear stabilizing control for ship-mounted cranes with disturbances induced by ship roll and heave movements: Design, analysis, and experiments. *IEEE Transactions on Systems, Man, and Cybernetics: Systems*. DOI: 10.1109/TSMC.2017.2700393
- [11] Sun N, Fang Y, Wu Y, Lu B. Nonlinear antiswing control of offshore cranes with unknown parameters and persistent ship-induced perturbations: Theoretical design and hardware experiments. *IEEE Transactions on Industrial Electronics*.
- [12] Singhose W, Kim D, Kenison M. Input shaping control of double-pendulum bridge crane oscillations. *Journal of Dynamic Systems, Measurement, and Control*. 2008;**130**(3):1-7
- [13] Grrido S, Abderrahim M, Gimnez A, Diez R, Balaguer C. Anti-swinging input shaping control of an automatic construction crane. *IEEE Transactions on Automation Science and Engineering*. 2008;**5**(3):549-557
- [14] Maghsoudi MJ, Mohamed Z, Tokhi MO, Husain AR, Abitdin MSZ. Control of a gantry crane using input-shaping schemes with distributed delay. *Transactions of the Institute of Measurement and Control*. 2017;**39**(3):361-370
- [15] Maghsoudi MJ, Mohamed Z, Sudin S, Buyamin S, Jaafar HI, Ahmad SM. An improved input shaping design for an efficient sway control of a nonlinear 3D overhead crane with friction. *Mechanical Systems and Signal Processing*. 2017;**92**:364-378
- [16] Sun N, Fang Y, Zhang X. Energy coupling output feedback control of 4-DOF underactuated cranes with saturated inputs. *Automatica*. 2013;**49**(5):1318-1325
- [17] Sun N, Fang Y. New energy analytical results for the regulation of underactuated overhead cranes: An end-effector motion-based approach. *IEEE Transactions on Industrial Electronics*. 2012;**59**(12):4723-4734
- [18] Tuan LA, Lee SG, Dang VH, Moon SC, Kim BS. Partial feedback linearization control of a three-dimensional overhead crane. *International Journal of Control, Automation and Systems*. 2013;**11**(4):718-727
- [19] Tuan LA, Kim GH, Kim MY, Lee SG. Partial feedback linearization control of overhead cranes with varying cable lengths. *International Journal of Precision Engineering and Manufacturing*. 2012;**13**(4):507-507

- [20] Tuan LA, Moon SC, Lee WG, Lee SG. Adaptive sliding mode control of the overhead crane with varying cable length. *Journal of Mechanical Science and Technology*. 2013;**27**(3):885-893
- [21] Lee LH, Huang CH, Ku SC, Yang ZH, Chang CY. Efficient visual feedback method to control a three-dimensional overhead crane. *IEEE Transactions on Industrial Electronics*. 2014;**61**(8):4073-4083
- [22] Almutairi NB, Zribi M. Sliding mode control of a three-dimensional overhead crane. *Journal of Vibration and Control*. 2009;**15**(11):1679-1730
- [23] Xi Z, Hesketh T. Discrete time integral sliding mode control for overhead crane with uncertainties. *IET Control Theory and Applications*. 2010;**4**(10):2071-2081
- [24] Bartolin G, Pisano A, Usai E. Second-order sliding-mode control of container cranes. *Automatica*. 2002;**38**:1783-1790
- [25] Ngo QH, Hong KS. Adaptive sliding mode control of container cranes. *IET Control Theory and Applications*. 2012;**6**(5):662-668
- [26] Sun N, Fang Y, Chen H, He B. Adaptive nonlinear crane control with load hoisting/lowering and unknown parameters: Design and experiments. *IEEE/ASME Transactions on Mechatronics*. 2015;**20**(5):2107-2119
- [27] Park MS, Chwa D, Eom M. Adaptive sliding-mode antisway control of uncertain overhead cranes with high-speed hoisting motion. *IEEE Transactions on Fuzzy Systems*. 2014;**22**(5):1262-1271
- [28] Sun N, Fang, Lu B, Fu Y. Slew/translation positioning and swing suppression for 4-DOF tower cranes with parametric uncertainties: Design and hardware experimentation. *IEEE Transactions on Industrial Electronics*. 2016;**63**(10):6407-6418
- [29] Zhao Y, Gao H. Fuzzy-model-based control of an overhead crane with input delay and actuator saturation. *IEEE Transactions on Fuzzy Systems*. 2012;**20**(1):181-186
- [30] Liu D, Yi J, Zhao D, Wang W. Adaptive sliding mode fuzzy control for a two-dimensional overhead crane. *Mechatronics*. 2005;**15**(5):505-522
- [31] Nakazono K, Ohnishi K, Kinjo H, Yamamoto T. Load swing suppression for rotary crane system using direct descent controller optimized by genetic algorithm. *Transactions of the Institute of Systems, Control and Information Engineers*. 2011;**22**(8):303-310
- [32] Lee LH, Huang PH, Shih YC, Chiang TC, Chang CY. Parallel neural network combined with sliding mode control in overhead crane control system. *Journal of Vibration and Control*. 2012;**20**(5):749-760
- [33] Uchiyama N, Ouyang H, Sano S. Simple rotary crane dynamics modelling and open-loop control for residual load sway suppression by only horizontal boom motion. *Mechatronics*. 2013;**23**(8):1223-1236

- [34] Sun N, Fang Y, Zhang X, Yuan Y. Transportation task-oriented trajectory planning for under-actuated overhead cranes using geometric analysis. *IET Control Theory and Applications*. 2012;6(10):1410-1423
- [35] Wu X, Xia X. Optimal motion planning for overhead cranes. *IET Control Theory and Applications*. 2014;8(17):1833-1842
- [36] Sun N, Fang Y, Zhang Y, Ma B. A novel kinematic coupling-based trajectory planning method for overhead cranes. *IEEE/ASME Transactions on Mechatronics*. 2012;17(1):166-173
- [37] Sun N, Wu Y, Fang Y, Chen H. Nonlinear antiswing control for crane systems with double-pendulum swing effects and uncertain parameters: Design and experiments. *IEEE Transactions on Automation Science and Engineering*. In press. DOI: 10.1109/TASE.2017.2723539
- [38] Sun N, Fang Y, Chen H, Lu B. Amplitude-saturated nonlinear output feedback antiswing control for underactuated cranes with double-pendulum cargo dynamics. *IEEE Transactions on Industrial Electronics*. 2017;64(3):2135-2146
- [39] Khalil HK. *Nonlinear Systems*. 3rd ed. Prentice Hall: Englewood Cliffs, NJ; 2002

IntechOpen

